Molecular Order and Disorder in the Frictional Response of Alkanethiol Self-Assembled Monolayers

ARTICLE *in* THE JOURNAL OF PHYSICAL CHEMISTRY A · MARCH 2011

Impact Factor: 2.69 · DOI: 10.1021/jp1121728 · Source: PubMed

3 AUTHORS, INCLUDING:

Nitya Nand Gosvami
University of Pennsylvania
39 PUBLICATIONS **448** CITATIONS
SEE PROFILE

Philip Egberts
The University of Calgary
23 PUBLICATIONS **169** CITATIONS
SEE PROFILE

THE JOURNAL OF PHYSICAL CHEMISTRY A

ARTICLE

pubs.acs.org/JPCA

Molecular Order and Disorder in the Frictional Response of Alkanethiol Self-Assembled Monolayers

Nitya Nand Gosvami,[†,‡] Philip Egberts,[†] and Roland Bennewitz*[,†]

[†]INM—Leibniz Institute for New Materials, Campus D2 2, 66123, Saarbrücken, Germany

[‡]Department of Chemistry, University College London, 20 Gordon Street, London WC1H 0AJ, United Kingdom

ABSTRACT: Molecular processes in the frictional response of an alkanethiol monolayer, self-assembled on a Au(111) surface, are studied by means of high-resolution friction force microscopy in ultrahigh vacuum. With increasing load, three regimes are observed on defect-free domains of the monolayer: smooth sliding with negligible friction, regular molecular stick−slip motion with increasing friction, and the onset of wear in the monolayer. Molecular contrast in the lateral force is found for inequivalent molecules within the unit cell of the c(4 × 2) superstructure. Significant differences in the frictional response are found between defect-free domains and areas including a domain boundary. Friction increases by an order of magnitude on domain boundaries in connection with irregular stick−slip motion. This increased friction at domain boundaries is observed at loads below the onset of wear.

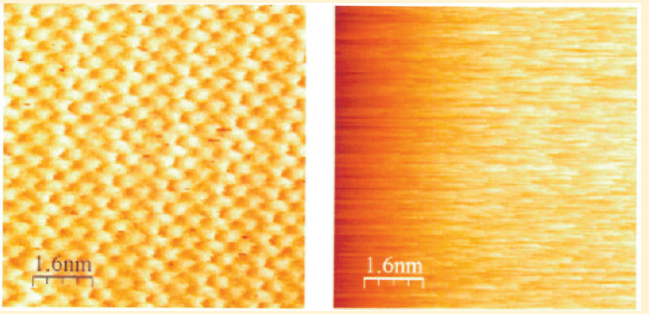

INTRODUCTION

Alkanethiols form layers with highly ordered structure and precise single molecular thickness on a variety of metal surfaces such as Au, Ag, or Cu, via a self-assembly processes.[1,2] These self-assembled monolayers (SAMs) are under rigorous investigations as they are easy to prepare and are promising candidates for a large variety of applications including modification of surface chemistry, corrosion protection, and colloidal chemistry.[2]

Particularly for tribological applications, SAMs are proposed as ideal boundary lubricants for small scale devices such as microelectromechanical systems, where oil-based lubricants cannot be used.[3−5] The interfacial properties of SAM-covered surfaces can be tailored by varying the chemistry of the headgroup of individual molecular units of the deposited monolayer, which allows tuning and control of wettability, adhesion, and friction and wear properties of the underlying substrate.[1,2] Owing to the high degree of order and the well-defined molecular thickness, SAMs also provide a unique system for fundamental studies of boundary lubrication, revealing tribological processes on molecular length scales. Despite more than two decades of work in tribology of SAMs,[5] some of the microscopic mechanisms are still under discussion. Open questions include the role of stick−slip motion on molecular scale, the load dependence of friction, the role of defects in the SAM, or the exact adsorption chemistry of the molecules on the substrate and its influence on lubrication.

The occurrence of molecular-scale stick−slip phenomena, possible key mechanisms for dissipation, in frictional sliding against a SAM is still debated in the literature. A recent review by Szlufarska et al.[5] concludes that the large pressure applied by a sharp tip during sliding results in the formation of gauche defects under the tip and splaying of molecules around the tip due to shear. These processes cause significant energy dissipation and prohibit coherent motion of the molecules and hence a stick−slip motion of the tip. There are a few reports of molecular-scale stick−slip on ordered layers of surfactant,[6] lipid,[7] and stearic acid molecules.[8] For alkanethiol SAMs on Au surfaces, which are the subject of our current study, to our knowledge no stick−slip measurements are reported although lateral force maps with molecular contrast have been presented.[9,10] Atomistic simulations of SAMs sliding against SAMs exhibited stick−slip instabilities on ordered alkanethiol SAMs, where packing and commensurability force a synchronized motion of the molecules.[11−14] In an atomistic simulation of a spring-loaded tip sliding on a SAM, Bonner and Baratoff observed a transition with increasing load from continuous sliding over stick−slip with the periodicity of the unit cell to irregular stick−slip.[15] Similarly, D'Acunto found in a simulation that periodic stick−slip occurs for a defect-free SAM and that lattice periodicity is lost upon onset of wear when stick−slip motion becomes irregular.[16]

Various effects have been found in experimental studies of the load dependence of friction on alkanethiol SAMs on Au surfaces. The results include the sublinear dependence expected from the contact size dependence in classical contact mechanics,[9] a

Special Issue: J. Peter Toennies Festschrift

Received: December 22, 2010
Revised: March 16, 2011
Published: March 28, 2011

stepwise increase of friction due to pressure-induced tilt of the molecules into interlocked positions,[17] a threshold behavior with a transition from low to high friction coefficients,[18] and a superlinear increase of friction caused by plowing of the tip in the SAM.[19] Atomistic simulations find a surprisingly consistent linear dependence of friction on load for SAMs.[14,20−23]

Defects such as domain boundaries, substrate pits, or molecular vacancies affect the frictional behavior of SAMs. Yang and Perry found that friction increases with defect density in SAMs.[24] It was also found that a dependence of friction on molecular chain length originates from the corresponding change in disorder in the SAM.[9] The interpretation was that disorder favors low-energy modes that are available to dissipation. This picture is confirmed in simulations which take disorder into account.[21,25,26]

An exact description of the adsorption chemistry for alkanethiol SAMs on Au(111) surface is still under development. Recent results indicate a significant reconstruction of the Au surface and an adsorption involving complexes of thiols and Au adatoms.[27−29] The interface between substrate and SAM can be expected to have a significant influence on the SAM structure and therefore on its frictional response. A direct consequence are friction contrasts between different superstructures of alkanethiol SAMs on Au(111) which have only recently been explored.[10,30,31]

These open questions have motivated our study on the frictional behavior of SAMs at the molecular level. We have employed high-resolution friction force microscopy in an ultrahigh vacuum environment on SAMs with large domains of perfect order in order to reveal molecular processes and to elucidate the role of domain boundary defects for friction. Working in ultrahigh vacuum also allows us to directly compare friction on SAMs with friction on the clean substrate metal surface. We present results for molecular stick−slip motion on decanethiol SAMs on Au(111) surfaces, the load dependence of the molecular friction in comparison to that on clean Au(111) surfaces, friction increase at domain boundaries, and molecularly resolved friction on the c(4 × 2) superstructure.

EXPERIMENTAL SECTION

The atomic force microscope (AFM) used for all experiments is a home-built instrument with the optical beam deflection method of force detection, operated in contact mode.[32] All measurements were conducted at room temperature under ultrahigh vacuum (UHV) conditions, where the pressure was lower than 2×10^{-10} mbar. Au(111) surfaces were prepared by thermally evaporating 300 nm thick polycrystalline films onto mica substrates in a vacuum evaporator (Oerlikon Leybold Vacuum GmbH, Univex 300) under high vacuum conditions (1×10^{-8} mbar). Following the deposition process, the gold films were annealed with a butane flame under atmospheric conditions to obtain atomically flat terraces with the (111) orientation of ∼200 nm size.[33]

The decanethiol SAM was prepared by immersing the Au(111) samples in 1.0 mM ethanolic solution of decanethiol for 2−4 h, while maintaining the solution temperature to ∼65 °C. This annealing step allows formation of large defect-free domains of 30−50 nm size,[34,35] suitable for AFM friction studies in completely defect-free regions of the monolayer but also near grain boundaries or pits on the flat Au(111) terraces. Such well-ordered SAMs exhibit an enhanced mechanical stability on the nanometer scale.[10] The solution was allowed to cool down to room temperature overnight. The samples were removed from the decanethiol solution, rinsed in pure ethanol, and dried under N_2 flow before mounting them to the sample holder and introducing them into the UHV chamber.

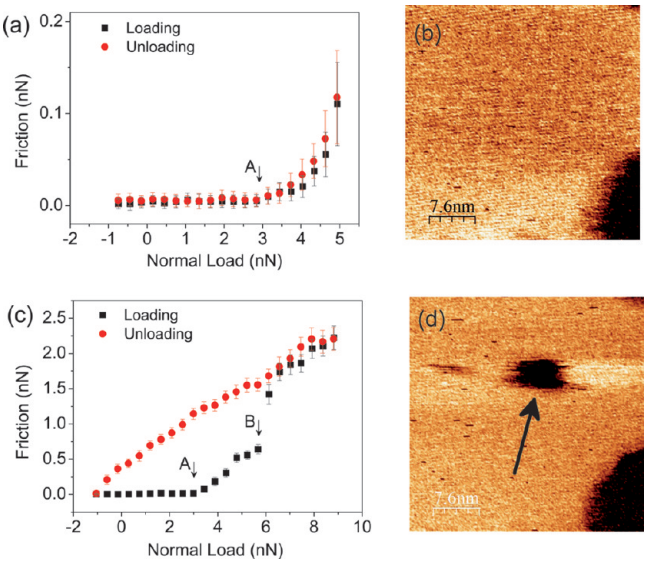

Figure 1. (a) Friction vs load curve recorded on a defect-free domain of the SAM. A reversible curve is obtained for loading and unloading with a maximum applied load of 5 nN. Label A indicates the transition load (∼3 nN) above which friction starts to increase with load. (b) Map of the surface after performing the experiment. (c) Friction vs load curve showing a large hysteresis between loading and unloading when exceeding the threshold load (∼6 nN) labeled B. The sharp increase in friction at B coincides with permanent damage to the SAM. (d) Map of the surface recorded after performing the experiment. The arrow indicates the area which was permanently damaged in the experiment described in (c), where an area of 8 × 8 nm^2 was tested. Maps in (b) and (d) show the normal force variation recorded while scanning at constant height over a domain of the SAM surface, after performing the friction vs load measurements.

Silicon cantilevers with an integrated tip (Nanosensors) were used as force sensors. The spring constant of these cantilevers in normal bending was 0.05−0.09 N/m and in torsion was 30−60 N/m. The stiffness of the cantilevers in both lateral twisting and normal bending was individually determined by the beam geometry method,[36,37] using the first normal resonant frequency to determine the thickness of the cantilever. Zero normal force is defined as an unbent cantilever, i.e., negative normal forces refer to a situation where the cantilever applies a normal force against the adhesion between tip and sample. Lateral forces are measured as twisting of the cantilever. Friction is determined as average of the lateral forces over many atomic rows in forward and backward scan. Quantitative friction results vary between different tips but are reproducible for the same tip. All results presented in this paper except Figure 3 have been recorded with the same tip but have been qualitatively reproduced with several different tips.

RESULTS AND DISCUSSION

The results of our experiments will be presented and discussed in the following order. We will start with the frictional response of a perfectly ordered SAM. The load dependence of friction will be related to the stick−slip pattern in lateral force maps and

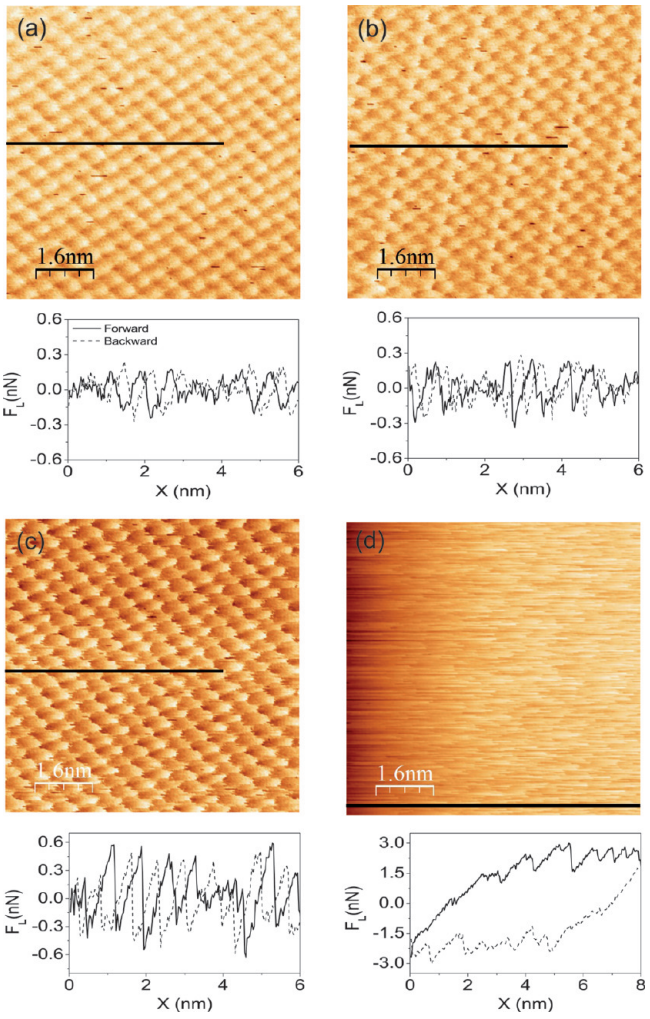

Figure 2. Lateral force maps recorded on a defect-free domain at different loads: (a) −0.5 nN, (b) 1.3 nN, (c) 4.3 nN, and (d) 6.6 nN. Molecular order and the c(4 × 2) superstructure can be recognized in (a−c). These and more frames have been evaluated for the data presented in panels a and c of Figure 1. Quantitative lateral force data are presented in representative cross sections recorded along the fast scan direction. Smooth sliding with symmetric molecular corrugation and negligible friction is observed in (a) and (b), whereas sawtooth-shaped molecular stick−slip is found in (c). Large friction and irregular stick−slip are observed for (d), causing permanent damage to the SAM.

discussed in comparison to atomic friction results for clean Au(111) surfaces. Molecular stick−slip patterns revealing the c(4 × 2) superstructure are then compared with recent work on the adsorption geometry of alkanethiols on Au(111). Finally, we will report the significant changes in the frictional response when including a domain boundary into the measured area.

Friction as a function of the applied load has been recorded on defect-free domains of the SAM and is plotted in Figure 1a. Very low friction of the order of 15 pN is found for normal loads between −1 nN and 3 nN. Friction does not change with load in this regime. For loads higher than 3 nN (the point of transition is labeled A) we observe an increase of friction with load, as it is generally expected for friction versus load experiments. The curve is perfectly reproduced upon unloading, indicating that any deformation of the film is fully reversible. When the normal load exceeds a tip-dependent threshold value, the film is permanently deformed or damaged and the friction versus load experiment is not reversible any more. An example is given in Figure 1c. A sharp rise in friction is observed at a load of ∼6 nN (the point of this transition is labeled B). The friction is significantly higher during unloading than during loading. It decreases almost linearly with load; the regime of constant low friction is not observed. The transitions marked A and B were reproducibly obtained at the same loads on different perfect SAM domains for a given tip.

The surface of the SAM was imaged at larger scale before and after each friction versus load experiment using very low loads in order to reveal any permanent changes in the surface structure (see Figure 1, panels b and d). No change in the SAM was observed for experiments in which the load was kept below 5 nN. However, a damaged region was observed for experiments in which the load exceeded this threshold. The measured depth of the damage is 1 nm, less than the film thickness. We believe that the damage reflects the removal of alkanethiol molecules rather than a substrate deformation. These results demonstrate that the irreversible transition B to higher friction in Figure 1c coincides with the onset of wear of the SAM.

Lateral force maps from the series of friction versus load experiments are shown in Figure 2. The molecular structure of the SAM can be clearly recognized in Figure 2a−c. For a load of 1.35 nN (Figure 2b) even the c(4 × 2) superstructure, which has been reported before for alkanethiol SAMs on Au(111),[10,29] becomes visible as modulation of the lateral force. No periodic structure is observed for Figure 2d, which was recorded at a load above the threshold B for the onset of wear. The development of molecular contrast with increasing load in the lateral force maps can be understood in terms of increasing interaction of the tip with the SAM. Initially, the weak corrugation of the lateral tip−surface potential reflects only the periodicity of the molecules. With increasing pressure, the potential reveals details of the c(4 × 2) superstructure which has been shown to reflect the bonding situation at the Au−SAM interface.[27−29] Further increase of the pressure Figure (2c) results in a enhancement of the molecular contrast but a loss of superstructure contrast. This development may be the result of change in tilt angle of the SAM molecules with increase in pressure.[9−16] Increasing the load also increases the contact area. When the contact area extends over several superstructure cells, the contrast of details within the superstructure is weakened due to averaging effects.

More quantitative details for the lateral force as a function of increasing load are provided in the individual lateral force loops in Figure 2. For loads below 3 nN (Figure 2a,b), a smooth modulation of the lateral force with the periodicity of the molecular film structure and almost negligible friction (i.e., average lateral force) is observed. Above the threshold *A* at a load of ∼3 nN, the lateral force shows a transition from smooth sliding with a symmetric appearance of the atomic corrugation to a sharp molecular stick−slip behavior, which appears as a sawtooth-shaped force curve in Figure 2c. Simultaneously, a clear offset of the lateral force curve indicates the onset of significant friction. This load dependence of lateral forces compares very well to experimental results reported by Socoliuc et al. for NaCl(001) surfaces, where a transition from smooth sliding with negligible friction to stick−slip motion with an increase in friction was observed for increasing loads.[38] In terms of a simple mechanical model, the transition from smooth sliding to dissipative stick−slip could be explained by the mechanical instabilities which occur once the curvature of the lateral surface

potential becomes larger than the stiffness of the spring pulling on the contact. Increasing the load will increase the corrugation of lateral surface potential, while the lateral stiffness of the tip apex stays almost constant. Therefore, an increase in load causes the transition to dissipative stick−slip.

Observation of sharp stick−slip events on the SAMs demonstrates that the monolayer behaves like a solid film under the large applied pressures. Furthermore, stick−slip indicates a coherent motion of molecules in contact with the sharp AFM tip which shears the film. On the basis of our data we can only suggest that the transition from smooth sliding to stick−slip also coincides with a penetration of the tip into the film. This interpretation has also been given by Houston et al., who observed a similar transition in the load dependence of friction.[18] Simulations by Bonner and Baratoff have similarly shown an onset of stick−slip once the tip penetrates the SAM.[15] The mechanisms described in this paragraph are comparable with the plowing process discussed by Flater et al. in order to explain a superlinear load dependence of friction on SAMs.[19] The sharp transition observed in the load versus friction curve in Figure 1a has been recorded with a sharp tip on a perfectly ordered film. We suggest that the sharp transition transforms into a smooth superlinear load dependence of friction when larger tips and less ordered films are studied, as in the study by Flater et al. We do not observe a stepwise increase of friction due to load-induced change in the packing of the SAM, which was observed by Barrena et al. on SAM islands.[39] In our case, further tilt is prevented by the complete coverage of the surface in a perfectly ordered film. Note that the friction in the smooth sliding regime for loads below transition A is not zero as expected in the oversimplified mechanical model. The finite friction can arise from dissipation of viscous character when the tip deforms the film during sliding without causing instabilities in the molecular order.

The friction loop recorded in the wear regime Figure (2d) shows high friction and strong irregular stick−slip behavior. It is in excellent agreement with a simulation study of an AFM tip sliding on a SAM surface, where periodic stick−slip is lost and friction increases as soon as wear starts.[16]

We now compare the load dependence of friction on the SAM surface to that of the underlying Au(111) surface. Friction experiments performed on clean Au(111) surfaces under the same conditions as in this study have revealed two regimes: stick−slip motion with negligible friction at low loads and irregular stick−slip with significant friction and wear above a threshold load of the order of a few nanonewtons.[33] The regime of stick−slip motion and of reversible increase in friction, which is observed between transitions A and B for SAMs on Au(111), is missing on clean Au(111) surfaces. We propose that the difference between the two cases lies in the contact formation. In the case of clean Au(111), a metallic neck between tip and surface is formed which mediates the low-friction stick−slip motion of the contact in form of a glide of Au(111) planes. When the load exceeds the threshold, the neck collapses and wear of the Au(111) surface sets in. The neck formation is confirmed in pull-off experiments, where the signatures of plastic deformation in metallic wire pulling are found in the force curves.[40] Such formation of a metallic neck is efficiently hindered by the SAM. We did not observe any plastic discontinuities in the pull-off curves recorded on the SAM-covered Au(111) surfaces. The pull-off forces were of the order of a few nanonewtons, much less than the typical values of about 100 nN found on on bare Au(111) surfaces. These observations demonstrate impressively

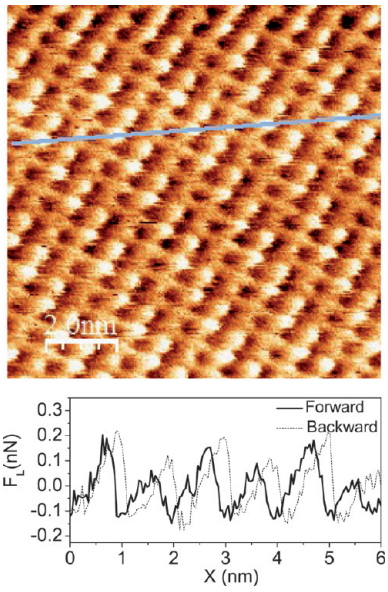

Figure 3. Lateral force map showing the c(4 × 2) superstructure with molecular resolution. The data were recorded at a load of −0.45 nN. Two molecular contrasts can be distinguished, as the tips interact differently with structurally inequivalent molecules. The lateral force curve taken from the map shows that the lateral force drop across different molecules within the superstructure cell differs by a factor of 2.

the mechanisms by which the Au(111) surface is fully passivated upon adsorption of the SAM,[41] leading to a stable sliding contact rather than an unstable metallic neck.

The observation of both the superstructure and the molecular periodicity in Figure 2b already points to the resolution power of atomic friction experiments. With exceptionally sharp tips, frictional processes at the molecular scale can be studied experimentally. An example is given in Figure 3 where the c(4 × 2) superstructure is resolved with single molecular resolution. This superstructure is composed of unit cells with four molecules. They are typically observed as inequivalent pairs of molecules.[29,42] Scanning tunneling microscopy of the superstructure provides a very small topographic contrast (∼30 pm) between the molecules.[42,43] However, the cross sections in Figure 3 demonstrate that the lateral force drop at the two inequivalent molecules can differ by a factor of 2. Only probes with sharp asperities, comparable in size to the superstructure periodicity, can detect such differences. The contrast may be enhanced by the small number of atoms whose contact forces contribute the largest part to the force acting on the sliding tip.[22] A full understanding of the lateral force contrast can only be obtained in atomistic simulations, which include the correct adsorption chemistry and structure of the superstructure.

We now discuss friction measurements which were recorded in a region where two differently oriented molecular domains meet in a domain boundary. A typical friction versus load curve is shown in Figure 4. Negligible friction is recorded for low loads, similar to a defect-free region of the SAM. However, friction increases sharply at a much smaller load (∼1 nN) than the transition A in Figure 1 for defect-free domains. Friction at a load of about 4 nN is by an order of magnitude higher compared to the defect-free region for similar normal loads. The result compares well to simulations in which defective SAMs exhibited higher

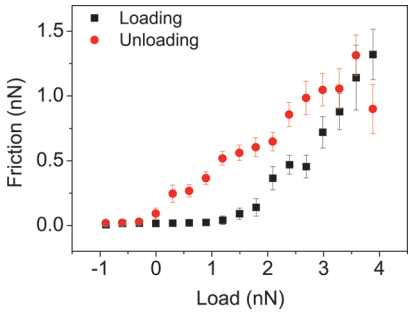

Figure 4. Friction vs load curve recorded on a region with a domain boundary. Compared to Figure 1, friction increases faster and at lower loads. The curve is not fully reversible for loading and unloading despite a maximum load below the threshold B. However, the low-friction regime at low loads is re-established upon unloading.

friction only at elevated loads.[25] Once the load is reduced during unloading, the friction curve shows some hysteresis. The hysteretic nature of friction and its increased values compared to the perfect SAM suggest a dissipative and disordering nature of the tip motion close to a grain boundary. Staying below threshold B for permanent damage of the SAM, Figure 4 reports a return of the friction value to very low values at low loads despite the hysteretic behavior found on the grain boundary. The recovery of the low friction regime indicates that the SAM was not permanently damaged in this experiment.

Lateral force maps of the region containing a grain boundary are shown in Figure 5. Orientational domains can be clearly distinguished by the different orientation of the molecular rows in panels a and b of Figure 5. Contrast in the lateral force can help to recognize domains of different orientations even when the superstructure is not resolved.[31] However, the average friction force does not show a contrast between different domains in our measurements. The fuzzy zone at the domain boundary in (a) has a width of about four molecular rows, giving an upper bound for the contact diameter and the size of the domain boundary, expected to be sharp for preparation at elevated temperatures.[43] In Figure 5b, a distortion of the molecular rows next to the domain boundary is observed at a load of 1.2 nN, or a load just above the onset of friction on domain boundaries. The lateral force map in Figure 5c, recorded at higher loads, shows a very fuzzy and irregular molecular structure where the original domain structure is almost completely obscured. Note that these experiments have been performed with the same tip as those reported in Figure 2, where we found perfect molecular order at comparable loads. All results could be reproduced repeatedly moving from perfect domains to domain boundaries and again to perfect domains, excluding tip wear as cause for the irregular structure in Figure 5c. After returning to low loads and to the low friction regime, molecular stick−slip can be again be observed as demonstrated in Figure 5d. The domain boundary appears to be slightly rearranged after the friction versus load experiment. However, there is no permanent damage comparable to the one seen in Figure 1d, which was caused by exceeding the load threshold B.

Quantitative examples for the lateral forces are plotted in the representative cross sections in Figure 5. Very low friction and smooth sliding are observed in panels a and d of Figure 5 at the lowest loads of 0.01 and −0.30 nN, whereas friction increases for all higher loads in panels b and c of Figure 5. Comparing the

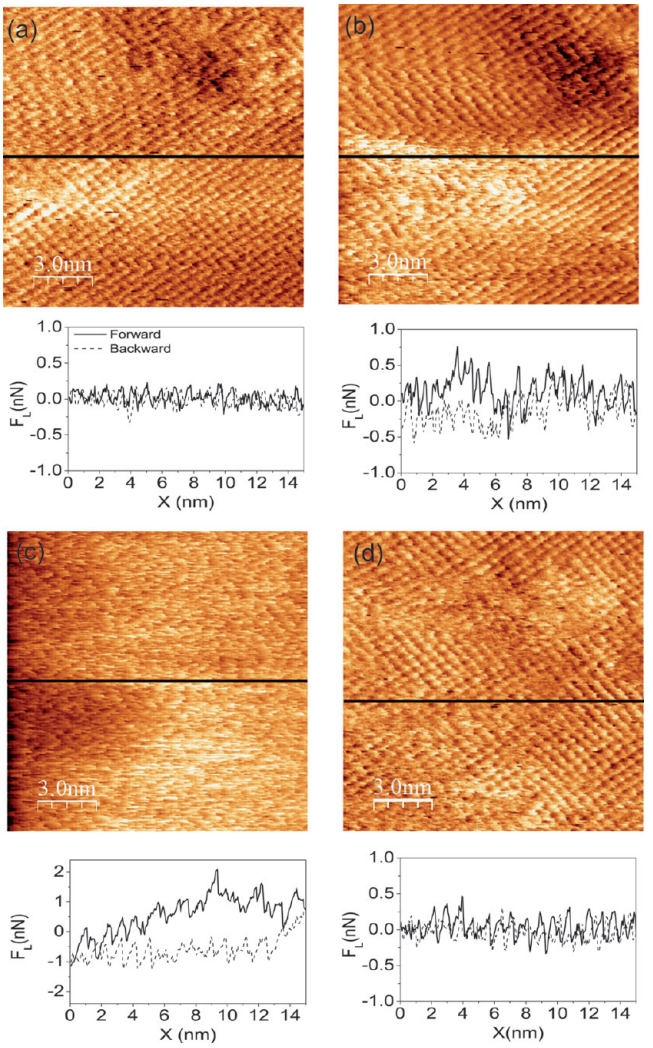

Figure 5. Lateral force maps recorded in a region where differently oriented domains meet. The domains can be recognized by the different orientation of molecular rows in (a) and (b), the domain boundary as brighter stripe of increased lateral force in (a). Maps have been recorded at the following loads: (a) 0.01 nN, (b) 1.2 nN, (c) 2.4 nN. The map in (d) has been recorded after unloading at a load of −0.3 nN. Quantitative lateral force data are presented in representative cross sections recorded along the fast scan direction. Smooth sliding with negligible friction is obtained for (a), whereas a sharp increase in friction and rather irregular stick−slip are observed for (b) and (c). The low friction and smooth sliding regime is re-established in (d).

lateral force curves in Figure 2 and in Figure 5, one finds not only the dramatic increase of friction on the domain boundary but also a much less regular stick−slip behavior. Domain boundaries are imperfections in the packing of the SAMs and provide open space. High friction and irregular tip motion suggest that these structural defects lead to the opening of other dissipative channels where molecules are easily splayed away from the tip apex under pressure and coherent motion of the molecules is compromised. These results are in general agreement with simulation and experimental studies, where imperfections in the SAM led to higher friction.[16,24−26] They demonstrate that domain boundaries in alkanethiol SAMs on Au contribute significantly to friction even before the film is worn.

SUMMARY

We have performed a high-resolution friction force microscopy study on alkanethiol self-assembled monolayers on Au(111) surfaces. Experiments on perfectly ordered SAM domains show a load-dependent transition from smooth sliding with negligible friction to regular molecular stick−slip with an increase in friction with load. The load dependence of friction is reversible unless a threshold for the onset of wear is exceeded. Molecular resolution of the stick−slip process reveals a strong contrast across the unit cell of a superstructure, indicating the importance of the interface structure which is under ongoing debate.

Significantly higher friction at lower loads is measured in areas of SAMs which include a boundary between domains of different molecular orientation. Irregular stick−slip is observed in these areas, but molecular order is always re-established when measuring at very low loads. These findings are in agreement with experimental and simulation studies where increased friction on defective SAMs is reported. Our results suggest that efforts have to be made toward minimizing the density of structural defects in SAM lubricant films in order to obtain stable contacts with ultralow friction. On the other hand, the stability of the films against wear is not affected as much as friction by domain boundaries.

AUTHOR INFORMATION

Corresponding Author

*E-mail: roland.bennewitz@inm-gmbh.de.

ACKNOWLEDGMENT

The authors thank Eduard Arzt for support of the project. N.N.G. acknowledges financial support by the Alexander von Humboldt Foundation.

REFERENCES

(1) Ulman, A. *Chem. Rev.* **1996**, *96*, 1533.
(2) Love, J.; Estroff, L.; Kriebel, J.; Nuzzo, R.; Whitesides, G. *Chem. Rev.* **2005**, *105*, 1103.
(3) Bhushan, B.; Israelachvili, J.; Landman, U. *Nature* **1995**, *374*, 607.
(4) Carpick, R.; Salmeron, M. *Chem. Rev.* **1997**, *97*, 1163.
(5) Szlufarska, I.; Chandross, M.; Carpick, R. W. *J. Phys. D: Appl. Phys.* **2008**, *41*, 123001.
(6) Liu, Y.; Wu, T.; Evans, D. *Langmuir* **1994**, *10*, 2241.
(7) Overney, R.; Takano, H.; Fujihira, M.; Paulus, W.; Ringsdorf, H. *Phys. Rev. Lett.* **1994**, *72*, 3546.
(8) Takano, H.; Fujihira, M. *J. Vac. Sci. Technol., B* **1996**, *14*, 1272.
(9) Lio, A.; Morant, C.; Ogletree, D. F.; Salmeron, M. *J. Phys. Chem. B* **1997**, *101*, 4767.
(10) Barrena, E.; Ocal, C. *J. Chem. Phys.* **1999**, *111*, 9797.
(11) Mikulski, P. T.; Harrison, J. A. *Carbon* **2001**, 6873.
(12) Zhang, T.; Wang, H.; Hu, Y. *Tribol. Lett.* **2003**, *14*, 69.
(13) Park, B.; Lorenz, C. D.; Chandross, M.; Stevens, M. J.; Grest, G. S.; Borodin, O. A. *Langmuir* **2004**, *20*, 10007.
(14) Hu, Y.; Zhang, T.; Ma, T.; Wang, H. *Comput. Mater. Sci.* **2006**, *38*, 98.
(15) Bonner, T.; Baratoff, A. *Surf. Sci.* **1997**, *377*−*379*, 1082.
(16) D'Acunto, M. *Nanotechnology* **2006**, *17*, 2954.
(17) Barrena, E.; Ocal, C.; Salmeron, M. *Surf. Sci.* **2001**, *482*, 1216.
(18) Houston, J.; Doelling, C.; Vanderlick, T.; Hu, Y.; Scoles, G.; Wenzl, I.; Lee, T. *Langmuir* **2005**, *21*, 3926.
(19) Flater, E. E.; Ashurst, W. R.; Carpick, R. W. *Langmuir* **2007**, *23*, 9242.
(20) Mikulski, P. T.; Herman, L. A.; Harrison, J. A. *Langmuir* **2005**, *21*, 12197.
(21) Chandross, M.; Lorenz, C. D.; Stevens, M. J.; Grest, G. S. *Langmuir* **2008**, *24*, 1240.
(22) Knippenberg, M. T.; Mikulski, P. T.; Dunlap, B. I.; Harrison, J. A. *Phys. Rev. B* **2008**, *78*, 235409.
(23) Knippenberg, M. T.; Mikulski, P. T.; Harrison, J. A. *Modell. Simul. Mater. Sci. Eng.* **2010**, *18*, 034002.
(24) Yang, X.; Perry, S. S. *Langmuir* **2003**, *19*, 6135.
(25) Mikulski, P.; Harrison, J. *J. Am. Chem. Soc.* **2001**, *123*, 6873.
(26) Chandross, M.; Webb, E.; Stevens, M.; Grest, G.; Garofalini, S. *Phys. Rev. Lett.* **2004**, *93*, 16.
(27) Voznyy, O.; Dubowski, J. J.; Yates, J. T., Jr.; Maksymovych, P. *J. Am. Chem. Soc.* **2009**, *131*, 12989.
(28) Gronbeck, H.; Odelius, M. *Phys. Rev. B* **2010**, *82*, 085416.
(29) Vericat, C.; Vela, M. E.; Benitez, G.; Carro, P.; Salvarezza, R. C. *Chem. Soc. Rev.* **2010**, *39*, 1805.
(30) Barrena, E.; Ocal, C.; Salmeron, M. *J. Chem. Phys.* **2001**, *114*, 4210.
(31) Munuera, C.; Barrena, E.; Ocal, C. *J. Phys. Chem. A* **2007**, *111*, 12721.
(32) Howald, L.; Meyer, E.; Lüthi, R.; Haefke, H.; Overney, R.; Rudin, H.; Güntherodt, H.-J. *Appl. Phys. Lett.* **1993**, *63*, 117.
(33) Gosvami, N. N.; Filleter, T.; Egberts, P.; Bennewitz, R. *Tribol. Lett.* **2009**, *39*, 19.
(34) Bucher, J.; Santesson, L.; Kern, K. *Langmuir* **1994**, *10*, 979.
(35) Cavalleri, O.; Hirstein, A.; Kern, K. *Surf. Sci.* **1995**, *340*, L960.
(36) Meyer, E.; Overney, R.; Dransfeld, K.; Gyalog, T. *Nanoscience: Friction and Rheology on the Nanometer Scale*; World Scientific: Singapore, 1998.
(37) Nonnenmacher, M.; Greschner, J.; Wolter, O.; Kassing, R. *J. Vac. Sci. Technol., B* **1991**, *9*, 1358.
(38) Socoliuc, A.; Bennewitz, R.; Gnecco, E.; Meyer, E. *Phys. Rev. Lett.* **2004**, *92*, 134301.
(39) Barrena, E.; Ocal, C.; Salmeron, M. *J. Chem. Phys.* **2000**, *113*, 2413.
(40) Bennewitz, R.; Brörmann, K.; Egberts, P.; Gosvami, N. N.; Hausen, F.; Held, C. *Adv. Eng. Mater.* **2010**, *12*, 362.
(41) Thomas, R. C.; Houston, J. E.; Michalske, T. A.; Crooks, R. M. *Science* **1993**, *259*, 1883.
(42) Poirier, G.; Tarlov, M. *Langmuir* **1994**, *10*, 2853.
(43) Lennartz, M. C.; Mueller-Meskamp, L.; Karthaeuser, S.; Waser, R. *Surf. Sci.* **2009**, *603*, 1156.